Extracting Anyon Statistics from Neural Network Fractional Quantum Hall States

Andres Perez Fadon [1,*] David Pfau [2] James S. Spencer [2] Wan Tong Lou [1]
Titus Neupert [3] and W. M. C. Foulkes [1]
[1] *Department of Physics, Imperial College London, London SW7 2AZ, United Kingdom*
[2] *DeepMind, London N1C 4DJ, United Kingdom*
[3] *Department of Physics, University of Zürich, Winterthurerstrasse 190, 8057 Zürich, Switzerland*

(Received 23 December 2025; accepted 28 July 2026; published 8 September 2026)

Fractional quantum Hall states host emergent anyons with exotic exchange statistics, but obtaining direct access to their topological properties in real systems remains a challenge. Neural network wave functions provide a flexible computational approach, as they can represent highly correlated states without requiring a tailored basis. Here, we use the neural network variational Monte Carlo method to study the fractional quantum Hall effect on the torus and find the three degenerate ground states at filling factor $\nu = 1/3$. From these, we extract the modular S-matrix via entanglement interferometry, a technique previously only applied to lattice models. The resulting S-matrix encodes the quantum dimensions, fusion rules, and exchange statistics of the emergent anyons, providing a direct numerical demonstration of the topological order. The calculated anyon properties match the well-known theoretical and experimental results. Our work establishes neural network wave functions as a powerful tool for investigating anyonic properties.

DOI: 10.1103/sb8g-qvn6

The fractional quantum Hall effect (FQHE) [1–9] arises when a strong magnetic field is applied to a two-dimensional (2D) layer of interacting electrons with a fractional Landau level filling factor ν. While the integer quantum Hall effect can be understood in terms of noninteracting electrons, the FQHE is intrinsically interaction driven and hosts anyonic excitations with fractional charge [2,10,11] and exchange statistics [4,12], which may be Abelian or non-Abelian [7,8,13,14]. The latter are of particular interest because of their potential use as decoherence-resistant qubits in topological quantum computing [15–17].

Computational studies of the FQHE have used exact diagonalization, density-matrix renormalization group methods, and variational trial wave functions. Most calculations are restricted to the lowest Landau level, either on the surface of a sphere [19–26] or in the plane with a disk of positive charge binding the electrons [2,20,27–29]. However, the assumption of vanishing Landau level mixing is not always valid, as fractional quantum Hall states have been seen for dimensionless mixing parameters up to $\kappa = 2.8$ [30]. In this limit, the assumption of vanishing Landau level mixing does not even approximately hold.

In recent years, neural wave functions [18,31–52] have proven able to provide accurate descriptions of a wide variety of interacting electron systems. Many of the aforementioned examples are strongly correlated and difficult to study with standard electronic structure methods because one lacks a many-body basis set that accurately captures the underlying physical phenomena, such as virtual positronium formation in positronic chemistry [46]. Neural networks, in contrast, are such expressive function approximators that, with only minor modifications, the same network architecture is capable of representing a wide range of correlated states accurately. Here, we show that neural wave functions are able to describe the topological order of quantum Hall states and can be used to study the properties of the emergent anyons.

The most interesting property of the FQHE ground state is that it has fractional excitations. The topological properties of these excitations are hard to investigate using direct computational methods, but several indirect approaches have been used to verify the topological order of fractional quantum Hall states obtained numerically. The first is to calculate the overlaps of the wave function with known topological states [19,53–56], on the assumption that the topological order is shared with the state that has the highest overlap. The second is to demonstrate an adiabatic connection. One can check numerically that the many-body gap remains open as, for instance, the Coulomb Hamiltonian H_0 is smoothly deformed to a Hamiltonian H_1 with a ground state of known topological order [57,58]. If this is true, the topological order of the ground state of H_0 is the same as that of the ground state of H_1. Entanglement entropy and, in particular, the entanglement spectrum contain fingerprints of the topological order [59,60]. Finally, some studies have calculated the braid phase by explicitly braiding the anyons [61,62].

This article reports the results of a neural-network-based variational Monte Carlo study of the fractional quantum

*Contact author: andres.perez-fadon19@imperial.ac.uk

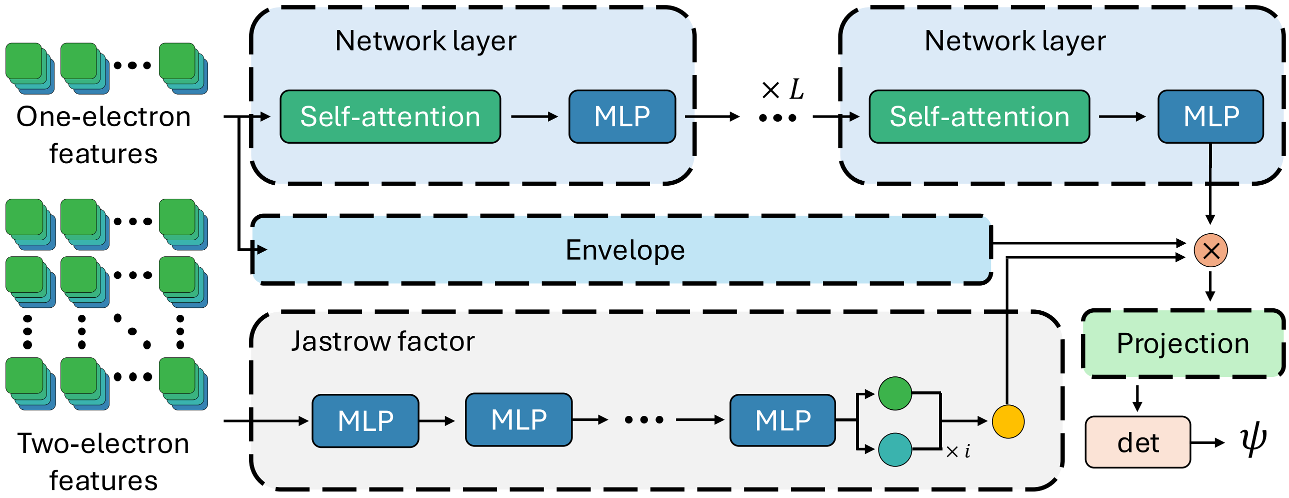

FIG. 1. Psiformer architecture with a custom complex-valued multilayer-perceptron-based Jastrow factor. The one-electron features depend on periodic functions of the position of each electron [18]. The Jastrow factor is evaluated independently for each pair of electrons. The values from each pair are then multiplied together. The envelope is a sum of quasiperiodic functions with learnable coefficients. The products of all components are reshaped into matrices in the so-called orbital projection layer, and the sum of the determinants of those matrices is the value of the wave function.

Hall effect at 1/3 filling on the torus. We calculate the three degenerate ground states and use them to directly obtain the modular S-matrix [63–68], which encodes the topological properties of the emergent anyons [69–72]. From the modular S-matrix, we calculate the quantum dimensions, fusion rules, and braid phase of the anyons. This is accomplished using entanglement interferometry, a method previously used for lattice systems [63,67].

Two other recent papers have used neural wave functions to simulate the FQHE in the continuum [26,29], but did not extract properties of the topological order. Lattice analogs of the FQHE, so-called fractional Chern insulators, have also been studied with neural network quantum states [73], but again the topological properties of the resulting wave functions were not considered.

The neural wave function we employ is based on the Psiformer architecture [42] as implemented in the FermiNet package [74], with most hyperparameters set to the default values. (For a complete list, see the Supplemental Material [75].) The Coulomb interactions were evaluated using 2D Ewald summations. We write our variational ansatz in Slater-Jastrow form,

$$\psi(\boldsymbol{r}_1,\ldots,\boldsymbol{r}_N) = J\sum_{d=1}^{N_{\mathrm{det}}} \det_{ij}\left[\phi_i^d(\boldsymbol{r}_j,\{\boldsymbol{r}_{/j}\})\right], \tag{1}$$

where J is a complex-valued Jastrow factor computed by a multilayer perceptron and the second term is the output of the Psiformer [42,74] (with the default Psiformer Jastrow factor removed). The structure of the wave function is shown schematically in Fig. 1. The orbitals $\phi_i^d(\boldsymbol{r}_j,\{\boldsymbol{r}_{/j}\})$ are expressed as

$$\phi_i^d(\boldsymbol{r}_j,\{\boldsymbol{r}_{/j}\}) = \varphi_i^d(\boldsymbol{r}_j,\{\boldsymbol{r}_{/j}\})\chi_i^d(\boldsymbol{r}_j), \tag{2}$$

where φ_i^d is a periodic function of all inputs obtained from the last layer of the network and χ_i^d is an envelope used to enforce the boundary conditions. We work in the Landau gauge, $\boldsymbol{A} = (yB, 0)^T$, with the magnetic field pointing into the xy plane. In the torus, this requires the use of quasiperiodic boundary conditions,

$$\psi(x + L_x, y) = \psi(x, y), \tag{3}$$

$$\psi(x, y + L_y) = e^{-i2\pi N_\phi x/L_x}\psi(x, y), \tag{4}$$

where L_x and L_y are the lengths of the sides of the toroidal simulation cell and $N_\phi = \frac{1}{\nu}N \in \mathbb{Z}$ is the number of flux quanta piercing the simulation cell. We write the envelope as a sum of quasiperiodic functions,

$$\chi_i^d(x, y) = \sum_{n=0}^{N_{\mathrm{LL}}-1}\sum_{s=0}^{N_\phi-1}\sigma_{ns}^{di} e_{ns}(x, y), \tag{5}$$

$$e_{ns}(x, y) = \sum_k f_{ns}\left(\frac{y}{L_y} + k\right)e^{i2\pi k N_\phi x/L_x}, \tag{6}$$

$$f_{ns}(a) = e^{-\pi N_\phi (a+s/N_\phi)^2} H_n(a + s/N_\phi), \tag{7}$$

where σ_{ns}^{di} are learnable parameters, H_n is the nth Hermite polynomial, and N_{LL} is a cutoff of Landau levels included. The form of the envelope is based on the eigenfunctions of a single particle moving on the torus subject to a magnetic field [76]. The complex-valued Jastrow factor J takes the form

$$J(\boldsymbol{r}_1,\ldots,\boldsymbol{r}_N) = \prod_{ij=1}^{N} \mathrm{MLP}(\boldsymbol{s}_i, \boldsymbol{s}_j, \boldsymbol{s}_{ij}, \boldsymbol{s}_{ij}), \tag{8}$$

where MLP stands for multilayer perceptron and $\boldsymbol{s}_i$ is a periodic function of $\boldsymbol{r}_i$ [18],

$$\boldsymbol{s}_i = \left(\cos\left(\frac{2\pi}{L}\boldsymbol{r}_i\right), \sin\left(\frac{2\pi}{L}\boldsymbol{r}_i\right)\right), \tag{9}$$

$$\boldsymbol{s}_{ij} = \left(\cos\left(\frac{2\pi}{L}(\boldsymbol{r}_i - \boldsymbol{r}_j)\right), \sin\left(\frac{2\pi}{L}(\boldsymbol{r}_i - \boldsymbol{r}_j)\right)\right), \tag{10}$$

TABLE I. Variational energies (in hartrees) obtained for the three lowest-energy eigenstates (lowest energies in bold). We use the shorthand FN+J to denote the combination of a FermiNet wave function with a complex MLP Jastrow factor, PS+J to denote the combination of a PsiFormer with a complex MLP Jastrow factor, and ED to denote exact diagonalization in the lowest Landau level. N is the number of electrons and B is the magnetic field in atomic units. For the four-electron case, we also calculated the energy of the fourth state, verifying that the ground state is threefold degenerate.

Ansatz	N	B	E_0	E_1	E_2	E_3
FN+J	4	10	**14.741 808(5)**	**14.741 909(6)**	**14.742 021(7)**	**14.879 138(9)**
PS+J	4	10	14.741 847(6)	14.741 960(7)	14.742 222(7)	14.879 14(1)
ED	4	10	14.748 217	14.748 227	14.748 228	14.897 403
Laughlin	4	10	14.761 14(2)	14.761 14(2)	14.761 14(2)	–
FN+J	5	5	7.882 24(1)	7.882 34(1)	7.882 43(1)	–
PS+J	5	5	**7.881 565(9)**	**7.881 872(9)**	**7.882 07(1)**	–
ED	5	5	7.886 53	7.886 53	7.886 53	–
Laughlin	5	5	7.889 23(2)	7.889 23(2)	7.889 23(2)	–
FN+J	6	5	9.470 78(2)	9.470 96(3)	9.472 10(3)	–
PS+J	6	5	**9.469 23(2)**	**9.469 35(2)**	**9.469 88(2)**	–
ED	6	5	9.473 84	9.473 85	9.473 85	–
Laughlin	6	5	9.478 03(2)	9.478 03(2)	9.478 03(2)	–
FN+J	8	5	12.649 81(5)	12.654 20(5)	12.661 93(7)	–
PS+J	8	5	**12.637 63(3)**	**12.637 87(3)**	**12.638 06(3)**	–
ED	8	5	12.641 98	12.641 99	12.642 00	–
Laughlin	8	5	12.649 35(2)	12.649 35(2)	12.649 35(2)	–

$$s_{ij} = \sum_{ab}\left[1-\cos\left(\frac{2\pi}{L_a}(r_{ij})_a\right)\right]M_{ab}\left[1-\cos\left(\frac{2\pi}{L_b}(r_{ij})_b\right)\right] + \sin\left(\frac{2\pi}{L_a}(r_{ij})_a\right)M_{ab}\sin\left(\frac{2\pi}{L_b}(r_{ij})_b\right), \tag{11}$$

where $a, b \in \{x, y\}$ and $M_{ab} = \boldsymbol{a}_a \cdot \boldsymbol{a}_b$, with $\boldsymbol{a}_j$ being the jth lattice vector of the torus. The fact that the Jastrow factor returns a complex output is essential, as it enables the network to represent the complex phase structure of the quantum Hall state.

As described above, the method used to calculate the quasiparticle properties requires the computation of multiple degenerate ground states. To maintain orthogonality, we use a penalty function method originally introduced for computing excited states [77]. The loss function is given by

$$\mathcal{L}[\{\psi_i\}] = \sum_i w_i E[\psi_i] + \lambda \sum_{i<j} |\mathcal{O}_{ij}|^2, \tag{12}$$

where $E[\psi]$ is the energy expectation value of ψ, $w_i \propto 1/i$, λ was chosen to be unity, and $\mathcal{O}_{ij}$ is the overlap between ψ_i and ψ_j. We find that the rate of convergence depends only weakly on the choice of ω_i and λ. Indeed, as we are targeting degenerate states, the method should converge regardless of the choice of these hyperparameters. As the method used to calculate the anyon properties requires access to the orthogonal ground states, the penalty method is more convenient than natural excited states [78], which would require further orthogonalization of the states. The parameters were optimized with the Kronecker factored approximate curvature (KFAC) algorithm [79].

The energies obtained from our calculations are reported in Table I. For the larger systems, the Psiformer [42] consistently obtains a lower energy than the earlier FermiNet architecture [34]. Using the variational principle to optimize neural network representations of FQHE wave functions proceeds smoothly but takes a surprisingly large amount of computer time (see the Supplemental Material [75]). This prevented us from studying systems with more than eight electrons. Previous neural wave function studies of the FQHE [26,29] were similarly limited. Further, these studies computed a single ground state in the sphere and disk geometry, respectively. The calculation of the entire degenerate space in the torus is a significant step up in complexity.

We are interested in the modular S-matrix, which contains topological information about the anyon excitations of the Hamiltonian. For example, the ground-state degeneracy of a system with N_a anyons of type a approaches $d_a^{N_a}$ for large N_a, where d_a is the quantum dimension of anyon type a. The total quantum dimension D is then defined by $D^2 = \sum_a d_a^2$, where the sum runs over all allowed anyon types in the theory. If one calculates the modular S-matrix, the quantum dimensions can be read from $S_{1a} = d_a/D$. Further, as there is always a "vacuum" particle with quantum dimension 1 (call it $a = e$), the total quantum dimension is $D = 1/S_{ee}$. The modular S-matrix can also be used to work out the fusion rules of the anyons via the Verlinde formula (see the Supplemental Material [75]). Further, if a and b are Abelian anyons, then $\arg(S_{ab})$ is the argument θ_{ab} of the complex phase obtained when braiding anyon a around anyon b [80].

To obtain the modular S-matrix, we follow the approach laid out in Ref. [63]. The first step is to use the penalty-function method [77] to find the number of degenerate ground states on the torus. The ground-state degeneracy is the number of quasiparticle types. For the $\nu = 1/3$ state, there are three anyon types: the vacuum/identity (e), the quasihole (qh), and the quasielectron (qe). Therefore, we expect the ground-state degeneracy to be three. Call the (orthonormal) degenerate ground states we converge to $|\xi_i\rangle$, $i \in \{1, 2, 3\}$.

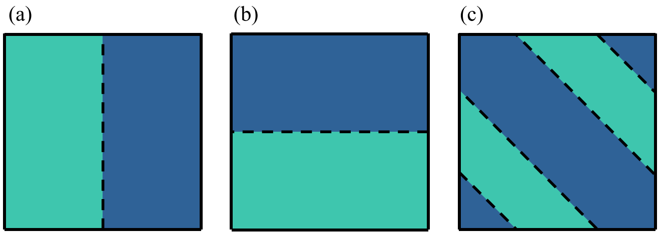

FIG. 2. Partitions across which the second Renyi entropy is calculated. Panels (a), (b), and (c) correspond to the partitions used to obtain $S_{\leftrightarrow}$, $S_{\updownarrow}$, and $S_{\swarrow\!\!\nearrow}$, respectively.

An arbitrary state in the degenerate subspace is a linear combination of $|\xi_i\rangle$:

$$|\psi\rangle = \sum_i \alpha_i |\xi_i\rangle. \tag{13}$$

Next, one finds the linear combination $|\Xi_1^{\leftrightarrow}\rangle$ that minimizes the second Renyi entropy, $S_R^{\leftrightarrow} = \ln[\mathrm{Tr}(\rho_A^2)]$, where ρ_A is the reduced density matrix in subregion A of the torus:

$$|\Xi_1^{\leftrightarrow}\rangle = \mathrm{argmin}_{|\psi\rangle} S_R^{\leftrightarrow}(\psi). \tag{14}$$

The symbol $\leftrightarrow$ refers to partitioning the torus horizontally, as shown in Fig. 2(a). The entropy is calculated using the method of Ref. [81], which we summarize in the Supplemental Material [75]. One then repeats the entropy minimization process to find a three-state basis, enforcing orthogonality with previous states:

$$|\Xi_2^{\leftrightarrow}\rangle = \mathrm{argmin}_{|\psi\rangle | \langle \Xi_1^{\leftrightarrow}|\psi\rangle = 0} S_R^{\leftrightarrow}(\psi), \tag{15}$$

$$|\Xi_3^{\leftrightarrow}\rangle = \mathrm{argmin}_{|\psi\rangle | \langle \Xi_1^{\leftrightarrow}|\psi\rangle = \langle \Xi_2^{\leftrightarrow}|\psi\rangle = 0} S_R^{\leftrightarrow}(\psi). \tag{16}$$

Similar bases are constructed by partitioning the system vertically, as shown in Fig. 2(b), to obtain $|\Xi_i^{\updownarrow}\rangle$, and diagonally, as shown in Fig. 2(c), to obtain $|\Xi_i^{\swarrow\!\!\nearrow}\rangle$. The modular S-matrix is then given by [67]

$$\begin{aligned} S = {} & \{R[(\bar{U}^{(\updownarrow)})^{-1}\bar{U}^{(\leftrightarrow)}]\}^{-1} R[(\bar{U}^{(\updownarrow)})^{-1}\bar{U}^{(\swarrow\!\!\nearrow)}] \\ & \times R[(\bar{U}^{(\swarrow\!\!\nearrow)})^{-1}\bar{U}^{(\leftrightarrow)}], \end{aligned} \tag{17}$$

where $R[X]$ denotes the matrix obtained after left and right multiplying X by the diagonal matrices of complex phases required to make the first row and column of X real and positive. The $\bar{U}$ matrices are defined as

$$\left|\Xi_b^{(\alpha)}\right\rangle = \bar{U}_{ab}^{(\alpha)} |\xi_a\rangle. \tag{18}$$

Note that although $\bar{U}_{ab}^{(\alpha)}$ is not invariant under $U(1)$ transformations of $|\xi_a\rangle$, the resulting S-matrix is.

The S-matrix computed from our eight-electron simulation was

$$\begin{aligned} S = {} & \frac{1}{\sqrt{3}} \begin{pmatrix} 1 & 1 & 1 \\ 1 & e^{i2\pi/3} & e^{-i2\pi/3} \\ 1 & e^{-i2\pi/3} & e^{i2\pi/3} \end{pmatrix} + \begin{pmatrix} +0.006+0.001i & -0.032-0.002i & +0.017+0.000i \\ +0.006-0.001i & +0.006+0.004i & -0.020+0.039i \\ -0.020-0.001i & +0.016-0.025i & -0.005-0.017i \end{pmatrix} \\ & \pm \begin{pmatrix} 0.035 & 0.025 & 0.034 \\ 0.032 & 0.043 & 0.034 \\ 0.032 & 0.045 & 0.042 \end{pmatrix} \pm \begin{pmatrix} 0.002 & 0.003 & 0.002 \\ 0.002 & 0.029 & 0.034 \\ 0.003 & 0.036 & 0.028 \end{pmatrix} i, \end{aligned} \tag{19}$$

where the first term is the expected result, the second term is the deviation from the expected result, and the last two terms are the statistical error of the mean calculated by computing the S-matrix 17 times. Let the anyon ordering corresponding to the rows and columns of the S-matrix be e, a, b (the entanglement interferometry method only gives the S-matrix up to a trivial permutation of the anyons' ordering sequence, so it is not possible to know whether a is the qh and b the qe, or vice versa). The total quantum dimension is estimated to be $D = 1/S_{ee} = \sqrt{3} + (0.001 - 0.004i) \pm 0.106 \pm 0.000i$. The other quantum dimensions can be calculated using $d_c = DS_{ce}$ and come out to be $d_a = 1.016 - 0.004i \pm 0.104 \pm 0.005i$, $d_b = 0.971 - 0.004i \pm 0.101 \pm 0.008i$ (note that we have assumed $d_e = 1$). For a list of the computed fusion rules, see the Supplemental Material [75]. The phases obtained by braiding different anyon types around each other were calculated to be $\theta_{a,a} = 2\pi/3 - 0.014 \pm 0.079$, $\theta_{b,b} = 2\pi/3 + 0.021 \pm 0.076$, and $\theta_{a,b} = -2\pi/3 - 0.013 \pm 0.051$ [obtained from averaging $\arg(S_{a,b})$ and $\arg(S_{b,a})$]. As shown in the Supplemental Material [75], S matrices computed for smaller systems also yield correct results, even for the tiny four-electron system. This is an important advantage of entanglement interferometry; it seems to produce the correct topological order even for very small systems, which would probably not be the case for entanglement scaling and entanglement spectroscopy. The reason, we suspect, is that the corrections are exponentially small in L/ℓ_{corr}, where $\ell_B = 1/\sqrt{B}$ is the magnetic length. Since $BL^2 = N_\phi \Phi_0 = N\Phi_0/\nu$, we find that $L/\ell_B = \sqrt{2\pi N/\nu}$. For the smallest system studied, containing only $N = 4$ electrons, $\exp(-L/\ell_B) \approx 10^{-4}$, implying that accurate results can already be obtained. We hope this will also be the case when studying more exotic phases, including non-Abelian systems.

In conclusion, this paper reported neural-network-based variational Monte Carlo simulations of the ground state of an FQHE system at filling fraction $\nu = 1/3$ in the torus, confirming that small modifications of existing neural wave functions make good ansätze for the quantum Hall problem. Using a penalty-function method [77], we demonstrated numerically that the ground state is threefold degenerate, corresponding to the three anyon types in the theory: the vacuum/identity (e), the quasihole (qh), and the quasielectron (qe). The three ground states in the torus were then used to extract the modular S-matrix through entanglement interferometry [63,67]. The modular S-matrix contains topological information about the emergent anyonic excitations and thus identifies the topological field theory corresponding to the ground state. We also obtained the quantum dimensions, fusion rules, and braid phases of the anyons. This was all done in the continuum with Landau level mixing, completely *ab initio* and assumption-free. We find that the topological anyon properties match those predicted by Wilczek and co-workers [4].

More generally, we have extended an assumption-free approach for calculating anyonic quasiparticle properties in lattice models to the continuum. Although we have investigated a system with known topological order, there is, in principle, no obstruction to using the same method for systems with unknown or debated topological order. This work has the potential to shed light on the nature of fractional quantum Hall states at other filling fractions and higher Landau levels, and may help understand the properties of other systems in which interactions lead to emergent anyonic excitations.

We thank Frank Schindler and Roberto Bondesan for helpful discussions. A.P.F.'s Ph.D. work was supported by the UK Engineering and Physical Sciences Research Council under Grant No. EP/W524323/1. This work was supported by a UKRI Future Leaders Fellowship MR/Y017331/1. The Gauss Centre for Supercomputing e.V. [82] is acknowledged for providing computing time through the John von Neumann Institute for Computing (NIC) on the GCS Supercomputer JUWELS at Jülich Supercomputing Centre (JSC), and the EUROfusion consortium for providing computing time on the Leonardo Supercomputer at CINECA in Bologna. The EUROfusion Consortium is funded by the European Union via the Euratom Research and Training Programme (Grant Agreement No. 101052200—EUROfusion). The authors acknowledge the use of resources provided by the Isambard-AI National AI Research Resource (AIRR) [83]. Isambard-AI is operated by the University of Bristol and is funded by the UK Government's Department for Science, Innovation and Technology (DSIT) via UK Research and Innovation, and the Science and Technology Facilities Council [ST/AIRR/I-A-I/1023]. T.N. acknowledges support from the Swiss National Science Foundation through a Quantum Grant (20QU-1_225225).

Views and opinions expressed are, however, those of the authors only and do not necessarily reflect those of the European Union or the European Commission. Neither the European Union nor the European Commission can be held responsible for them.

The software used to generate the data in the manuscript is openly available in a public repository [85]. Further details are provided in the Supplemental Material [75].

[1] D. C. Tsui, H. L. Stormer, and A. C. Gossard, Two-dimensional magnetotransport in the extreme quantum limit, Phys. Rev. Lett. **48**, 1559 (1982).

[2] R. B. Laughlin, Anomalous quantum Hall effect: An incompressible quantum fluid with fractionally charged excitations, Phys. Rev. Lett. **50**, 1395 (1983).

[3] F. D. M. Haldane, Fractional quantization of the Hall effect: A hierarchy of incompressible quantum fluid states, Phys. Rev. Lett. **51**, 605 (1983).

[4] D. Arovas, J. R. Schrieffer, and F. Wilczek, Fractional statistics and the quantum Hall effect, Phys. Rev. Lett. **53**, 722 (1984).

[5] F. D. M. Haldane and E. H. Rezayi, Finite-size studies of the incompressible state of the fractionally quantized Hall effect and its excitations, Phys. Rev. Lett. **54**, 237 (1985).

[6] J. K. Jain, Composite-fermion approach for the fractional quantum Hall effect, Phys. Rev. Lett. **63**, 199 (1989).

[7] G. Moore and N. Read, Nonabelions in the fractional quantum Hall effect, Nucl. Phys. B **360**, 362 (1991).

[8] E. H. Rezayi and F. D. M. Haldane, Incompressible paired Hall state, stripe order, and the composite fermion liquid phase in half-filled Landau levels, Phys. Rev. Lett. **84**, 4685 (2000).

[9] J. K. Jain, *Composite Fermions* (Cambridge University Press, Cambridge, 2007).

[10] R. De-Picciotto, M. Reznikov, M. Heiblum, V. Umansky, G. Bunin, and D. Mahalu, Direct observation of a fractional charge, Physica B **249–251**, 395 (1998).

[11] L. Saminadayar, D. Glattli, Y. Jin, and B. Etienne, Observation of the $e/3$ fractionally charged Laughlin quasiparticle, Phys. Rev. Lett. **79**, 2526 (1997).

[12] F. Wilczek, Magnetic flux, angular momentum, and statistics, Phys. Rev. Lett. **48**, 1144 (1982).

[13] M. Greiter, X.-G. Wen, and F. Wilczek, Paired Hall states, Nucl. Phys. B **374**, 567 (1992).

[14] K. K. W. Ma, M. R. Peterson, V. W. Scarola, and K. Yang, Fractional quantum Hall effect at the filling factor $\nu = 5/2$, in *Encyclopedia of Condensed Matter Physics*, edited by T. Chakraborty (Editor-in-Chief of the 2nd ed.; Section Editors were A. M. Sanchez, H. Aoki, R. H. Blick, R. Raimondi, R. A. Roemer, and V. M. Fomin (Academic Press, San Diego, CA, 2024), Vol. 1, pp. 324–365.

[15] C. Nayak, S. H. Simon, A. Stern, M. Freedman, and S. Das Sarma, Non-Abelian anyons and topological quantum computation, Rev. Mod. Phys. **80**, 1083 (2008).

[16] A. Y. Kitaev, Fault-tolerant quantum computation by anyons, Ann. Phys. **303**, 2 (2003).

[17] L. S. Georgiev, Topological quantum computation with non-abelian anyons in fractional quantum hall states, in *Quantum Systems in Physics, Chemistry, and Biology: Advances in Concepts and Applications*, edited by A. Tadjer, R. Pavlov, J. Maruani, E. J. Brändas, and G. Delgado-Barrio (Springer, Cham, 2017), pp. 75–94.

[18] G. Cassella, H. Sutterud, S. Azadi, N. D. Drummond, D. Pfau, J. S. Spencer, and W. M. C. Foulkes, Discovering quantum phase transitions with fermionic neural networks, Phys. Rev. Lett. **130**, 036401 (2023).

[19] R. H. Morf, Transition from quantum Hall to compressible states in the second Landau level: New light on the $\nu = 5/2$ enigma, Phys. Rev. Lett. **80**, 1505 (1998).

[20] X. Wan, Z.-X. Hu, E. Rezayi, and K. Yang, Fractional quantum Hall effect at $\nu = 5/2$: Ground states, non-Abelian quasiholes, and edge modes in a microscopic model, Phys. Rev. B **77**, 165316 (2008).

[21] A. Feiguin, E. Rezayi, C. Nayak, and S. Das Sarma, Density matrix renormalization group study of incompressible fractional quantum Hall states, Phys. Rev. Lett. **100**, 166803 (2008).

[22] D. Kovrizhin, Density matrix renormalization group for bosonic quantum Hall effect, Phys. Rev. B **81**, 125130 (2010).

[23] J. Zhao, D. Sheng, and F. Haldane, Fractional quantum Hall states at 13 and 52 filling: Density-matrix renormalization group calculations, Phys. Rev. B **83**, 195135 (2011).

[24] M. Arciniaga and M. R. Peterson, Landau level quantization for massless Dirac fermions in the spherical geometry: Graphene fractional quantum Hall effect on the Haldane sphere, Phys. Rev. B **94**, 035105 (2016).

[25] Z.-W. Zuo, A. C. Balram, S. Pu, J. Zhao, T. Jolicoeur, A. Wójs, and J. Jain, Interplay between fractional quantum Hall liquid and crystal phases at low filling, Phys. Rev. B **102**, 075307 (2020).

[26] Y. Qian, T. Zhao, J. Zhang, T. Xiang, X. Li, and J. Chen, Describing Landau level mixing in fractional quantum Hall states with deep learning, Phys. Rev. Lett. **134**, 176503 (2025).

[27] R. Morf and B. Halperin, Monte Carlo evaluation of trial wave functions for the fractional quantized Hall effect: Disk geometry, Phys. Rev. B **33**, 2221 (1986).

[28] Z.-X. Hu, Z. Papić, S. Johri, R. N. Bhatt, and P. Schmitteckert, Comparison of the density-matrix renormalization group method applied to fractional quantum Hall systems in different geometries, Phys. Lett. A **376**, 2157 (2012).

[29] Y. Teng, D. D. Dai, and L. Fu, Solving the fractional quantum Hall problem with self-attention neural network, Phys. Rev. B **111**, 205117 (2025).

[30] N. Samkharadze, D. Ro, L. Pfeiffer, K. West, and G. Csáthy, Observation of an anomalous density-dependent energy gap of the $\nu = 5/2$ fractional quantum Hall state in the low-density regime, Phys. Rev. B **96**, 085105 (2017).

[31] G. Carleo and M. Troyer, Solving the quantum many-body problem with artificial neural networks, Science **355**, 602 (2017).

[32] K. Choo, A. Mezzacapo, and G. Carleo, Fermionic neural-network states for *ab-initio* electronic structure, Nat. Commun. **11**, 2368 (2020).

[33] J. Hermann, Z. Schätzle, and F. Noé, Deep-neural-network solution of the electronic Schrödinger equation, Nat. Chem. **12**, 891 (2020).

[34] D. Pfau, J. S. Spencer, A. G. Matthews, and W. M. C. Foulkes, *Ab initio* solution of the many-electron Schrödinger equation with deep neural networks, Phys. Rev. Res. **2**, 033429 (2020).

[35] J. S. Spencer, D. Pfau, A. Botev, and W. M. C. Foulkes, Better, faster fermionic neural networks, arXiv:2011.07125.

[36] N. Gao and S. Günnemann, *Ab-initio* potential energy surfaces by pairing GNNs with neural wave functions, arXiv:2110.05064.

[37] X. Li, Z. Li, and J. Chen, *Ab initio* calculation of real solids via neural network ansatz, Nat. Commun. **13**, 7895 (2022).

[38] X. Li, C. Fan, W. Ren, and J. Chen, Fermionic neural network with effective core potential, Phys. Rev. Res. **4**, 013021 (2022).

[39] G. Pescia, J. Han, A. Lovato, J. Lu, and G. Carleo, Neural-network quantum states for periodic systems in continuous space, Phys. Rev. Res. **4**, 023138 (2022).

[40] Y. Qian, W. Fu, W. Ren, and J. Chen, Interatomic force from neural network based variational quantum Monte Carlo, J. Chem. Phys. **157**, 164104 (2022).

[41] M. Scherbela, R. Reisenhofer, L. Gerard, P. Marquetand, and P. Grohs, Solving the electronic Schrödinger equation for multiple nuclear geometries with weight-sharing deep neural networks, Nat. Comput. Sci. **2**, 331 (2022).

[42] I. von Glehn, J. S. Spencer, and D. Pfau, A self-attention ansatz for *ab-initio* quantum chemistry, arXiv:2211.13672.

[43] M. T. Entwistle, Z. Schätzle, P. A. Erdman, J. Hermann, and F. Noé, Electronic excited states in deep variational Monte Carlo, Nat. Commun. **14**, 274 (2023).

[44] N. Gao and S. Günnemann, Generalizing neural wave functions, in *International Conference on Machine Learning, Honolulu, Hawaii, USA* (PMLR, 2023), pp. 10708–10726.

[45] J. Hermann, J. Spencer, K. Choo, A. Mezzacapo, W. M. C. Foulkes, D. Pfau, G. Carleo, and F. Noé, *Ab initio* quantum chemistry with neural-network wavefunctions, Nat. Rev. Chem. **7**, 692 (2023).

[46] G. Cassella, W. Foulkes, D. Pfau, and J. S. Spencer, Neural network variational Monte Carlo for positronic chemistry, Nat. Commun. **15**, 5214 (2024).

[47] X. Li, Y. Qian, and J. Chen, Electric polarization from a many-body neural network ansatz, Phys. Rev. Lett. **132**, 176401 (2024).

[48] W. T. Lou, H. Sutterud, G. Cassella, W. M. C. Foulkes, J. Knolle, D. Pfau, and J. S. Spencer, Neural wave functions for superfluids, Phys. Rev. X **14**, 021030 (2024).

[49] G. Pescia, J. Nys, J. Kim, A. Lovato, and G. Carleo, Message-passing neural quantum states for the homogeneous electron gas, Phys. Rev. B **110**, 035108 (2024).

[50] Y. Qian, X. Li, and J. Chen, Force and stress calculations with a neural-network wave function for solids, Faraday Discuss. **254**, 529 (2024).

[51] M. Scherbela, L. Gerard, and P. Grohs, Towards a transferable fermionic neural wavefunction for molecules, Nat. Commun. **15**, 120 (2024).

[52] A. Perez Fadon, G. Cassella, H. Sutterud, and W. Foulkes, Interaction-induced symmetry breaking in circular quantum dots, J. Chem. Phys. **162**, 154305 (2025).

[53] M. R. Peterson, Y.-L. Wu, M. Cheng, M. Barkeshli, Z. Wang, and S. Das Sarma, Abelian and non-Abelian states in $\nu = 2/3$ bilayer fractional quantum Hall systems, Phys. Rev. B **92**, 035103 (2015).

[54] K. Pakrouski, M. R. Peterson, T. Jolicoeur, V. W. Scarola, C. Nayak, and M. Troyer, Phase diagram of the $\nu = 5/2$ fractional quantum Hall effect: Effects of Landau-level mixing and nonzero width, Phys. Rev. X **5**, 021004 (2015).

[55] J.-S. Jeong and K. Park, Bilayer mapping of the paired quantum Hall state: Instability toward anisotropic pairing, Phys. Rev. B **91**, 195119 (2015).

[56] E. H. Rezayi, Landau level mixing and the ground state of the $\nu = 5/2$ quantum Hall effect, Phys. Rev. Lett. **119**, 026801 (2017).

[57] M. Storni, R. H. Morf, and S. Das Sarma, Fractional quantum Hall state at $\nu = \frac{5}{2}$ and the Moore-Read Pfaffian, Phys. Rev. Lett. **104**, 076803 (2010).

[58] W. Hutzel, J. J. McCord, P. T. Raum, B. Stern, H. Wang, V. W. Scarola, and M. R. Peterson, Particle-hole-symmetric model for a paired fractional quantum Hall state in a half-filled Landau level, Phys. Rev. B **99**, 045126 (2019).

[59] H. Li and F. D. M. Haldane, Entanglement spectrum as a generalization of entanglement entropy: Identification of topological

order in non-Abelian fractional quantum Hall effect states, Phys. Rev. Lett. **101**, 010504 (2008).
[60] R. S. Mong, M. P. Zaletel, F. Pollmann, and Z. Papić, Fibonacci anyons and charge density order in the 12/5 and 13/5 quantum Hall plateaus, Phys. Rev. B **95**, 115136 (2017).
[61] E. Prodan and F. D. M. Haldane, Mapping the braiding properties of the Moore-Read state, Phys. Rev. B **80**, 115121 (2009).
[62] M. Storni and R. Morf, Localized quasiholes and the Majorana fermion in fractional quantum Hall state at $\nu = \frac{5}{2}$ via direct diagonalization, Phys. Rev. B **83**, 195306 (2011).
[63] Y. Zhang, T. Grover, A. Turner, M. Oshikawa, and A. Vishwanath, Quasiparticle statistics and braiding from ground-state entanglement, Phys. Rev. B **85**, 235151 (2012).
[64] L. Cincio and G. Vidal, Characterizing topological order by studying the ground states on an infinite cylinder, Phys. Rev. Lett. **110**, 067208 (2013).
[65] W. Zhu, D. N. Sheng, and F. D. M. Haldane, Minimal entangled states and modular matrix for fractional quantum Hall effect in topological flat bands, Phys. Rev. B **88**, 035122 (2013).
[66] W. Zhu, S. Gong, F. Haldane, and D. Sheng, Identifying non-Abelian topological order through minimal entangled states, Phys. Rev. Lett. **112**, 096803 (2014).
[67] Y. Zhang, T. Grover, and A. Vishwanath, General procedure for determining braiding and statistics of anyons using entanglement interferometry, Phys. Rev. B **91**, 035127 (2015).
[68] Z. Li and R. S. Mong, Detecting topological order from modular transformations of ground states on the torus, Phys. Rev. B **106**, 235115 (2022).
[69] B. Bakalov and A. A. Kirillov, *Lectures on Tensor Categories and Modular Functors* (American Mathematical Society, Providence, RI, 2001), Vol. 21.
[70] C. Kassel, *Quantum Groups* (Springer Science & Business Media, New York, 2012), Vol. 155.
[71] V. G. Turaev, *Quantum Invariants of Knots and 3-Manifolds* (de Gruyter, Berlin, 2010).
[72] S. H. Simon, *Topological Quantum* (Oxford University Press, Oxford, 2023).
[73] X. Li, Y. Chen, B. Li, H. Chen, F. Wu, J. Chen, and W. Ren, Deep Learning sheds light on integer and fractional topological insulators, arXiv:2503.11756.
[74] J. S. Spencer and D. Pfau, FermiNet code repository, 2020, http://github.com/deepmind/ferminet.
[75] See Supplemental Material at http://link.aps.org/supplemental/10.1103/sb8g-qvn6 for the network architecture and training hyperparameters, the derivation of the fusion rules, additional numerical results for smaller electron numbers, and details of the Rényi entropy estimator used to compute the modular S matrix, which includes Ref. [84].
[76] M. Fremling, Modular covariance properties of composite fermions on the torus, Phys. Rev. B **99**, 075126 (2019).
[77] W. A. Wheeler, K. G. Kleiner, and L. K. Wagner, Ensemble variational Monte Carlo for optimization of correlated excited state wave functions, Electron. Struct. **6**, 025001 (2024).
[78] D. Pfau, S. Axelrod, H. Sutterud, I. von Glehn, and J. S. Spencer, Accurate computation of quantum excited states with neural networks, Science **385**, eadn0137 (2024).
[79] J. Martens and R. Grosse, Optimizing neural networks with Kronecker-factored approximate curvature, in *Proceedings of the 32nd International Conference on Machine Learning, Lille, France* (PMLR, 2015), Vol. 37, pp. 2408–2417.
[80] D. Delmastro and J. Gomis, Symmetries of Abelian Chern-Simons theories and arithmetic, J. High Energ. Phys. 03 (2021) 006.
[81] N. M. Tubman and J. McMinis, Renyi entanglement entropy of molecules: Interaction effects and signatures of bonding, arXiv:1204.4731.
[82] www.gauss-centre.eu.
[83] S. McIntosh-Smith, S. R. Alam, and C. Woods, Isambard-AI: A leadership class supercomputer optimised specifically for artificial intelligence, arXiv:2410.11199.
[84] M. B. Hastings, I. González, A. B. Kallin, and R. G. Melko, Measuring Renyi entanglement entropy in quantum Monte Carlo simulations, Phys. Rev. Lett. **104**, 157201 (2010).
[85] A. Perez Fadon, D. Pfau, J. S. Spencer, W. T. Lou, T. Neupert, and W. M. C. Foulkes, Code for “Extracting anyon statistics from neural network fractional quantum Hall states” [Software], GitHub, 2026, https://github.com/APerezFadon/ferminet_fqhe_new.